Big Bang nucleosynthesis with a non-Maxwellian distribution

C. A. Bertulani[1,2], J. Fuqua[2] and M.S. Hussein[3]
[1] *GSI Helmholtzzentrum für Schwerionenforschung, D-64291 Darmstadt, Germany*
[2] *Texas A&M University-Commerce, Commerce, TX 75429-3011, USA*
[3] *Instituto de Estudos Avançados, Universidade de São Paulo, C.P. 72.012, 05508-970, São Paulo, Brazil and Instituto de Física, Universidade de São Paulo, C. P. 66318, 05389-970 São Paulo, Brazil*

The abundances of light elements based on the big bang nucleosynthesis model are calculated using the Tsallis non-extensive statistics. The impact of the variation of the non-extensive parameter q from the unity value is compared to observations and to the abundance yields from the standard big bang model. We find large differences between the reaction rates and the abundance of light elements calculated with the extensive and the non-extensive statistics. A large deviation of the non-extensive parameter from $q = 1$ (corresponding to Boltzmann statistics) does not seem to be compatible with observations.

I. INTRODUCTION

The cosmological big bang model has made seminal predictions relevant for our understanding of the universe, many of which have been spectacularly confirmed by observation. The model is the only probe of physics in the early universe during the interval from $3-20$ min, after which the temperature and density of the universe fell below that which is required for nuclear fusion and prevented elements heavier than beryllium from forming. One of the most celebrated predictions of the model is the cosmic microwave background (CMB) radiation temperature of 2.275 K [1]. The model has also provided strict constraints and guidance to other areas of science, such as nuclear and particle physics. One of the constraints set by the model is the number of light neutrino families, predicted to be $N_\nu = 3$. From the measurement of the Z_0 width by LEP experiments at CERN one knows now that $N_\nu = 2.9840 \pm 0.0082$ [2].

In the big bang model nearly all neutrons end up in ^{4}He, so that the relative abundance of ^{4}He depends on the number of neutrino families and also on the neutron lifetime τ_n (which the big bang model sets at about 886 s). The neutron-lifetime, important for weak reaction rates has been measured in nuclear physics laboratories to high precision (885.7 ± 0.8) s, in excellent agreement with the predictions of the big bang model [3].

The baryonic density of the universe deduced from the observations of the anisotropies of the CMB radiation, constrains the value of the number of baryons per photon, η, which remains constant during the expansion of the universe. Big bang model predictions also agree with the experimentally deduced value of from WMAP observations, $\eta = 6.16 \pm 0.15 \times 10^{-10}$ [4].

Of our interest in this work is the abundances of light elements in big bang nucleosynthesis. At the very early stages (first 20 min) of the universe evolution, when it was dense and hot enough for nuclear reactions to take place, the temperature of the primordial plasma decreased from a few MeV down to about 10 keV, light nuclides as ^{2}H, ^{3}He, ^{4}He and, to a smaller extent, ^{7}Li were produced via a network of nuclear processes, resulting into abundances for these species which can be determined with several observational techniques and in different astrophysical environments. Apparent discrepancies for the Li abundances in metal poor stars, as measured observationally and as inferred by WMAP, have promoted a wealth of new inquiries on Big Bang Nucleosynthesis (BBN) and on stellar mixing processes destroying Li, whose results are not yet final. Further studies of light-element abundances in low metallicity stars and extragalactic H II regions, as well as better estimates from BBN models are required to tackle this issue, integrating high resolution spectroscopic studies of stellar and interstellar matter with nucleosynthesis models and nuclear physics experiments and theories [5].

One of the basic assumptions to calculate the nuclear reaction rates during the BBN is the Maxwell-Boltzmann distribution of the kinetic energy of the nuclei. This distribution follows the concept that the kinetic energy of the nuclei present in the primordial plasma are determined by the classical Boltzmann statistics. The same assumption is used in nucleosynthesis during stellar evolution. Recently, an increasing number of experiments, theoretical developments, have challenged the Boltzmann-Gibbs description of statistical mechanics. It seems that the Boltzmann-Gibbs is not adequate for systems with long range interactions, and with memory effects. Therefore, it was unavoidable that new approaches for the Boltzmann-Gibbs formalism were proposed. Nowadays, a very popular approach is based on the proposal by Tsallis [6], herewith denoted as *non-extensive statistics*. Statistical mechanics assumes that energy is an "extensive" variable, meaning that the total energy of the system is proportional to the system size; similarly the entropy is also supposed to be extensive. This might be justified due to the short-range nature of the interactions which hold matter together. But if one deals with long-range interactions, most prominently gravity; one can then find that energy is not extensive.

Tsallis proposed that to calculate the average values of some quantities, such as the energy of the system, the number of molecules, the volume it occupies, etc, one searches for the probability distribution which maximizes the entropy, subject to the constraint that it gives

the right average values of those quantities. He then proposed to replace the usual (Gibbs) entropy with a new, non-extensive quantity, now commonly called the Tsallis entropy, and maximize that, subject to usual constraints. There is actually a whole infinite family of Tsallis entropies, indexed by a real-valued parameter q, which quantifies the degree of departure from extensivity (one gets the usual entropy back again when $q = 1$). It was shown in many circumstances that the classical results of statistical mechanics can be translated into the new theory [7].

In the next sections, we shown that the Maxwell-Boltzmann distribution, a cornerstone of the big bang and stellar evolution nucleosynthesis, is strongly modified by the non-extensive statistics. As a consequence, it also affects strongly the outcome of the BBN. Based on the successes of the big bang model, it is fair to assume that our results set strong constraints on the limits of the parameter q used in non-extensive statistics. Attempts to solve the lithium problem has assumed all sorts of "new physics" [5]. This one adds to the list of new attempts, although our results imply a much wider impact on BBN as expected for the solution of the lithium problem. As we show in the next sections, a strong deviation from $q = 1$ is very unlikely, based on comparison of observations and the BBN model.

II. MAXWELLIAN AND NON-MAXWELLIN DISTRIBUTIONS

Nuclear reaction rates in the BBN and in stelar evolution are strongly dependent of the particle velocity distributions. The fusion reaction rates for nuclear species 1 and 2 is given by $\langle\sigma v\rangle_{12}$, i.e., an average of the fusion cross section of 1+2 with their relative velocity, described by a velocity distribution. It is thus worthwhile to study the modifications of the stellar reaction rates due to the modifications introduced by the non-extensive statistics.

A. Non-extensive Statistics

Statistical systems in equilibrium are described by the Boltzmann-Gibbs entropy,

$$\mathcal{S}_{BG} = -k_B \sum_i p_i \ln p_i, \tag{1}$$

where k_B is the Boltzmann constant, and p_i is the probability of the i-th microstate. For two independent systems A, B, the probability of the system $A+B$ being in a state $i + j$, with i a microstate of A and j a microstate of B, is

$$p_{i+j}^{A+B} = p_i^A \cdot p_j^B. \tag{2}$$

Therefore, the Boltzmann-Gibbs entropy satisfies the relation

$$\mathcal{S}_{A+B} = \mathcal{S}_A + \mathcal{S}_B. \tag{3}$$

Thus, the entropy based on the Boltzmann-Gibbs statistic is an *extensive* quantity.

In the non-extensive statistics [6], one replaces the traditional entropy by the following one:

$$\mathcal{S}_q = k_B \frac{1 - \sum_i p_i^q}{q - 1}, \tag{4}$$

where q is a real number. For $q = 1$, $\mathcal{S}_q = \mathcal{S}_{BG}$. Thus, the Tsallis statistics is a natural generalization of the Boltzmann-Gibbs entropy.

Now it follows that

$$\mathcal{S}_q(A + B) = \mathcal{S}_q(A) + \mathcal{S}_q(B)_(1 - q)\mathcal{S}_q(A)\mathcal{S}_q(B). \tag{5}$$

The variable q is a measure of the *non-extensivity*. Tsallis has shown that a formalism of statistical mechanics can be consistently developed in terms of this generalized entropy [7].

A consequence of the non- extensive formalism is that the distribution function which maximizes S_q is non-Maxwellian [8–10]. For $q = 1$, the Maxwell distribution function is reproduced. But for $q < 1$, high energy states are more probable than in the extensive case. On the other hand, for $q > 1$ high energy states are less probable than in the extensive case, and there is a cutoff beyond which no states exist.

B. Maxwellian Distribution

In stars, the thermonuclear reaction rate with a Maxwellian distribution is given by [11]

$$R_{ij} = \frac{N_i N_j}{1+\delta_{ij}}\langle\sigma v\rangle = \frac{N_i N_j}{1+\delta_{ij}}\left(\frac{8}{\pi\mu}\right)^{\frac{1}{2}}\left(\frac{1}{k_B T}\right)^{\frac{3}{2}} \times \int_0^\infty dE S(E) \exp\left[-\left(\frac{E}{k_B T} + 2\pi\eta(E)\right)\right], \tag{6}$$

where σ is the fusion cross section, v is the relative velocity of the ij-pair, N_i is the number of nuclei of species i, μ is the reduced mass of $i+j$, T is the temperature, $S(E)$ is the astrophysical S-factor, and $\eta = Z_i Z_j e^2/\hbar v$ is the Sommerfeld parameter, with Z_i the i-th nuclide charge and $E = \mu v^2/2$ is the relative energy of $i + j$.

The energy dependence of the reaction cross sections is usually expressed in terms of the equation

$$\sigma(E) = \frac{S(E)}{E} \exp\left[-2\pi\eta(E)\right]. \tag{7}$$

We write $2\pi\eta = b/\sqrt{E}$, where

$$b = 0.9898 Z_i Z_j \sqrt{A}\ \mathrm{MeV}^{1/2}, \tag{8}$$

where A is the reduced mass in amu. The factor $1 + \delta_{ij}$ in the denominator of Eq. (6) corrects for the double-counting when $i = j$. The S-factor has a relatively weak dependence on the energy E, except when it is close to a resonance, where it is strongly peaked.

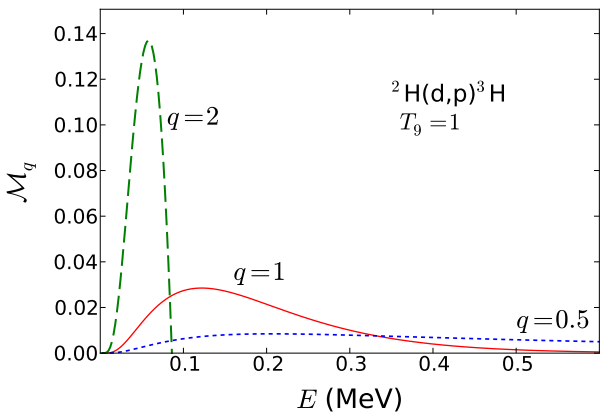

Figure 1: Modified Gamow distributions $\mathcal{M}_q(E,T)$ of deuterons relevant for the reaction ^{2}H(d,p)^{3}H at $T_9 = 1$. The solid line, for $q = 1$, corresponds to the use of a Maxwell-Boltzmann distribution. Also shown are the results when using non-extensive distributions for $q = 0.5$ (dotted line) and $q = 2$ (dashed line).

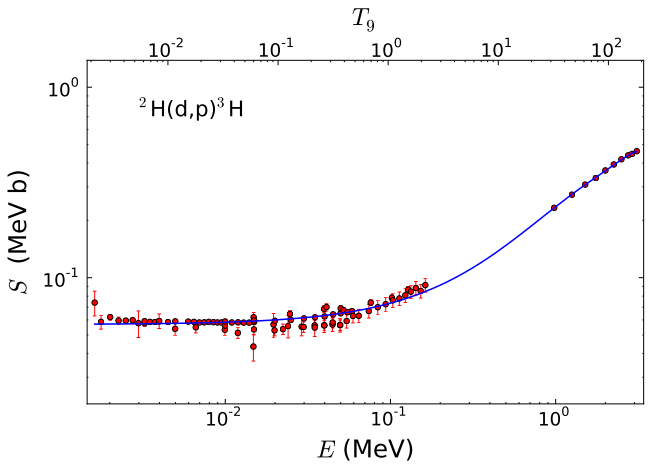

Figure 2: S-factor for the reaction ^{2}H(d,p)^{3}H as a function of the relative energy E and of the temperature T_9. The data are from Refs. [12–16]. The solid curve is a polynomial fit to the experimental data.

C. Non-Maxwellian Distribution

The non-extensive description of the Maxwell-Boltzmann distribution corresponds to the substitution $f(E) \to f_q(E)$, where [7]

$$f_q(E) = \left(1 - \frac{q-1}{k_B T} E\right)^{\frac{1}{q-1}} \xrightarrow{q\to 1} \exp\left(-\frac{E}{k_B T}\right), \quad 0 < E < \infty. \tag{9}$$

If $q - 1 < 0$, Eq. (9) is real for any value of $E \geq 0$. However, if $q - 1 > 0$, $f(E)$ is real only if the quantity in square brackets is positive. This means that

$$0 \leq E \leq \frac{k_B T}{q-1}, \quad \text{if} \quad q \geq 1$$
$$0 \leq E, \quad \text{if} \quad q \leq 1. \tag{10}$$

Thus, in the interval $0 < q < 1$ one has $0 < E < \infty$ and for $1 < q < \infty$ one has $0 < E < E_{\max} = k_B T/(q-1)$.

With this new statistics, the reaction rate becomes

$$R_{ij} = \frac{N_i N_j}{1+\delta_{ij}} I_q, \tag{11}$$

and the rate integral, $I(q)$, is given by

$$I_q = \int_0^{E_{max}} dE S(E) \mathcal{M}_q(E,T), \tag{12}$$

where the "modified" Gamow energy distribution is

$$\mathcal{M}_q(E,T) = \mathcal{A}(q,T)\left(1 - \frac{q-1}{k_B T} E\right)^{\frac{1}{q-1}} e^{-b/\sqrt{E}}$$
$$= \mathcal{A}(q,T)\left(1 - \frac{q-1}{0.08617 T_9} E\right)^{\frac{1}{q-1}}$$
$$\times \exp\left[-0.9898 Z_i Z_j \sqrt{\frac{A}{E}}\right] \tag{13}$$

is the non-extensive Maxwell velocity distribution, $E_{max} = \infty$ for $0 < q < 1$ and $E_{\max} = k_B T/(1-q)$ for $1 < q < \infty$, and E in MeV units. $\mathcal{A}(q,T)$ is a normalization constant which depends on the temperature and the non-extensive parameter q.

III. REACTION RATES DURING BIG BANG NUCLEOSYNTHESIS

In figure 1 we plot the Gamow energy distributions of deuterons relevant for the reaction ^{2}H(d,p)^{3}H at $T_9 = 1$. The solid line, for $q = 1$, corresponds to the use of the Maxwell-Boltzmann distribution. Also shown are results for non-extensive distributions for $q = 0.5$ (dotted line) and $q = 2$ (dashed line). One observes that for $q < 1$, higher kinetic energies are more accessible than in the extensive case ($q = 1$). For $q > 1$ high energies are less probable than in the extensive case, and there is a cutoff beyond which no kinetic energy is reached. In the example shown in the figure for $q = 2$, the cutoff occurs at 0.086 MeV, or 86 keV.

We will explore the modifications of the BBN elemental abundances due to a variation of the non-extensive

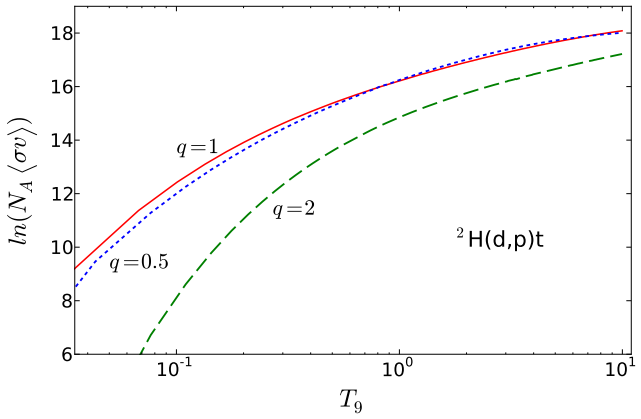

Figure 3: Reaction rates for ^{2}H(d,p)^{3}H as a function of the temperature T_9 for different values of the non-extensive parameter q. The rates are given in terms of the natural logarithm of $N_A\langle\sigma v\rangle$ (in units of cm^3 mol^{-1} s^{-1}). Results with the use of non-extensive distributions for $q = 0.5$ (dotted line) and $q = 2$ (dashed line) are shown.

statistics parameter q. We will express our reaction rates in the form $N_A\langle\sigma v\rangle$ (in units of cm^3 mol^{-1} s^{-1}), where N_A is the Avogadro number and $\langle\sigma v\rangle$ involves the integral in Eq. (6) with the Maxwell distribution $f(E)$ replaced by Eq. (9). First we show how the reaction rates are modified for $q \neq 1$.

In figure 2 we show the S-factor for the reaction ^{2}H(d,p)^{3}H as a function of the relative energy E. Also shown is the dependence on T_9 (temperature in units of 10^9 K) for the effective Gamow energy

$$E = E_0 = 0.122(Z_i^2 Z_j^2 A)^{1/3} T_9^{2/3} \text{ MeV}, \qquad (14)$$

where A is the reduced mass in amu. The data are from Refs. [12–16] and the solid curve is a chi-square polynomial function fit to the data.

Using the chi-square polynomial fit obtained to fit the data presented in figure 2, we show in figure 3 the reaction rates for ^{2}H(d,p)^{3}H as a function of the temperature T_9 for two different values of the non-extensive parameter q. The integrals in equation (12) are performed numerically. For charge particles, a good accuracy (witihin 0.1%) is reached using the integration limits between $E_0 - 5\Delta E$ and $E_0 + 5\Delta E$, where ΔE is given by Eq. (15) below. The rates are expressed in terms of the natural logarithm of $N_A\langle\sigma v\rangle$ (in units of cm^3 mol^{-1} s^{-1}). The solid curve corresponds to the usual Maxwell-Boltzman distribution, i.e., $q = 1$. The dashed and dotted curves are obtained for $q = 2$ and $q = 0.5$, respectively. In both cases, we see deviations from the Maxwellian rate. For $q > 1$ the deviations are rather large and the tendency is an overall suppression of the reaction rates, specially at low temperatures. This effect arises from the non-Maxwellian energy cutoff which for this reaction occurs at $0.086T_9$ MeV and which prevents a great number of reactions to occur at higher energies.

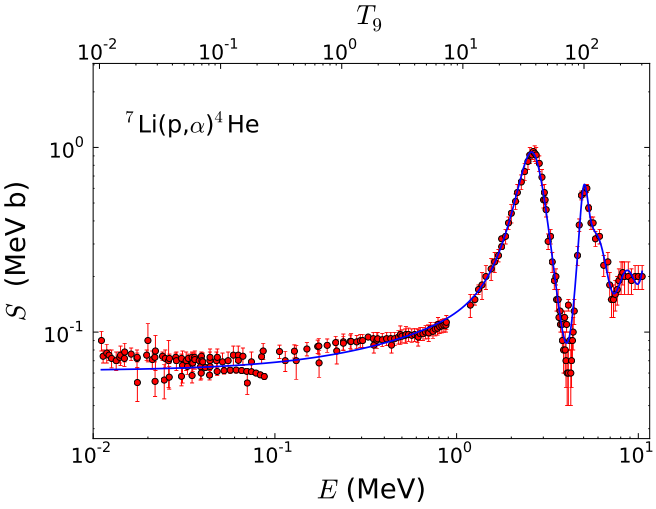

Figure 4: S-factor for the reaction ^{7}Li(p,α)^{4}He as a function of the relative energy E and of T_9. The data are from Refs. [17–27]. The solid curve is a chi-square function fit to the data using a sum of polynomials plus Breit-Wigner functions.

For $q < 1$ the nearly similar result as with the Maxwell-Boltzmann distribution is due to a competition between suppression in reaction rates at low energies and their enhancement at high energies. The relevant range of energies is set by the Gamow energy which for a Maxwellian distribution is given by Eq. (14) and by the energy window,

$$\Delta E = 0.2368(Z_i^2 Z_j^2 A)^{1/6} T_9^{5/6} \text{ MeV}, \qquad (15)$$

which for the reaction ^{2}H(d,p)^{3}H amounts to $0.2368T_9^{5/6}$ MeV. This explains why, at $T_9 = 1$, the range of relevant energies for the calculation of the reaction rate is shown by the solid curve in figure 1. For $q < 1$ the Gamow window ΔE is larger and there is as much a contribution from the suppression of reaction rates at low energies compared to the Maxwell-Boltzmann distribution, as there is a corresponding enhancement at higher energies. This explains the nearly equal results shown in figure 3 for $q = 1$ and $q < 1$. This finding applies to all charged particle reaction rates, except for those when the S-factor has a strong dependence on energy at, and around, $E = E_0$. But no such behavior exists for the most important charged induced reactions in the BBN (neutron-induced reactions will be discussed separately).

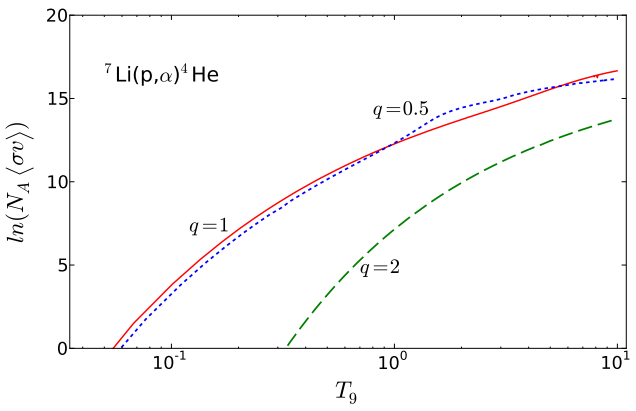

Figure 5: Reaction rates for ^{7}Li(p,α)^{4}He as a function of the temperature T_9 for two different values of the non-extensive parameter q. The rates are given in terms of the natural logarithm of $N_A\langle\sigma v\rangle$ (in units of cm^3 mol^{-1} s^{-1}). Results with the use of non-extensive distributions for $q = 0.5$ (dotted line) and $q = 2$ (dashed line) are shown.

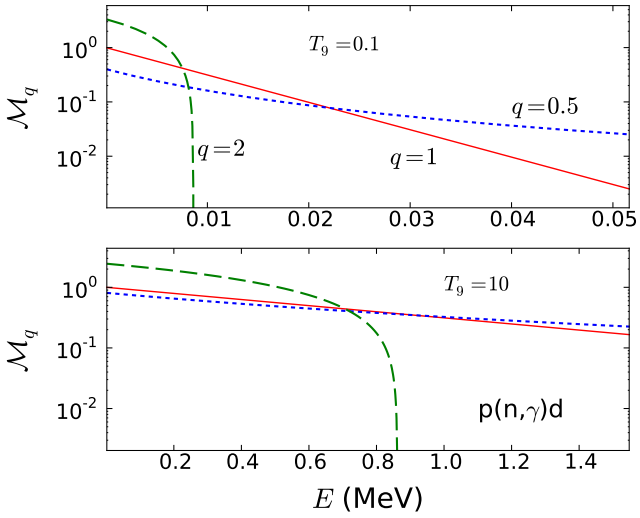

Figure 6: Spectral function $\mathcal{M}_q(E,T)$ for protons and neutrons relevant for the reaction p(n,γ)d at $T_9 = 0.1$ (upper panel) and $T_9 = 10$ (lower panel). The solid line, for $q = 1$, corresponds to the usual Boltzmann distribution. Also shown are non-extensive distributions for $q = 0.5$ (dotted line) and $q = 2$ (dashed line).

The findings described above for the reaction ^{2}H(d,p)^{3}H are not specific but apply to all charged particles of relevance to the BBN. We demonstrate this with one more example: the ^{7}Li(p,α)^{4}He reaction, responsible for ^{7}Li destruction. In figure 4 we show the S-factor for this reaction as a function of the relative energy E. One sees prominent resonances at higher energies. Also shown in the figure is the dependence of the reaction on T_9. The data are from Refs. [17–27] and the solid curve is a chi-square function fit to the data using a sum of polynomials plus Breit-Wigner functions.

Using the chi-square function fit obtained to fit the data presented in figure 4, we show in figure 5 the reaction rates for ^{7}Li(p,α)^{4}He as a function of the temperature T_9 for two different values of the non-extensive parameter q. The rates are given in terms of the natural logarithm of $N_A\langle\sigma v\rangle$ (in units of cm^3 mol^{-1} s^{-1}). The solid curve corresponds to the usual Maxwell-Boltzman distribution, i.e., $q = 1$. The dashed and dotted curves are obtained for $q = 2$ and $q = 0.5$, respectively. As with the case presented in figure 3, in both cases we see deviations from the Maxwellian rate. But, as before, for $q = 2$ the deviations are larger and the tendency is a strong suppression of the reaction rates as the temperature decreases. It is interesting to note that the non-Maxwellian rates for $q = 0.5$ are more sensitive to the resonances than for $q > 1$. This is because, as seen in figure 1, for $q < 1$ the velocity distribution is spread to considerably larger values of energies, being therefore more sensitive to the location of high energy resonances.

We now turn to neutron induced reactions, which are only a few cases of high relevance for the BBN, notably the p(n,γ)d, ^{3}He(n,p)t, and ^{7}Be(n,p)^{7}Li reactions. For neutron induced reactions, the cross section at low energies is usually proportional to $1/v$, where $v = \sqrt{2mE}/\hbar$ is the neutron velocity. Thus, it is sometimes appropriate to rewrite Eq. (7) as

$$\sigma(E) = \frac{S(E)}{E} = \frac{R(E)}{\sqrt{E}} \tag{16}$$

where $R(E)$ is a slowly varying function of energy similar to an S-factor. The distribution function within the reaction rate integral (12) is also rewritten as

$$\mathcal{M}_q(E,T) \; = \mathcal{A}(q,T) f_q(E) = \; \mathcal{A}(q,T) \left(1 - \frac{q-1}{k_B T} E\right)^{\frac{1}{q-1}} . \tag{17}$$

The absence of the tunneling factor $\exp(-b/\sqrt{E})$ in Eq. (17) inhibts the dependence of the reaction rates on the non-extensive parameter q.

In figure 6 we plot the kinetic energy distributions of nucleons relevant for the reaction p(n,γ)d at $T_9 = 0.1$ (upper panel) and $T_9 = 10$ (lower panel). The solid line, for $q = 1$, corresponds to the usual Boltzmann distribution. Also shown are results for the non-extensive distributions for $q = 0.5$ (dotted line) and $q = 2$ (dashed line). One observes that, as for the charged particles case, with $q < 1$ higher kinetic energies are more probable than in the extensive case ($q = 1$). With $q > 1$ high energies are less accessible than in the extensive case, and there is a cutoff beyond which no kinetic energy is reached. A noticeable difference form the case of charged

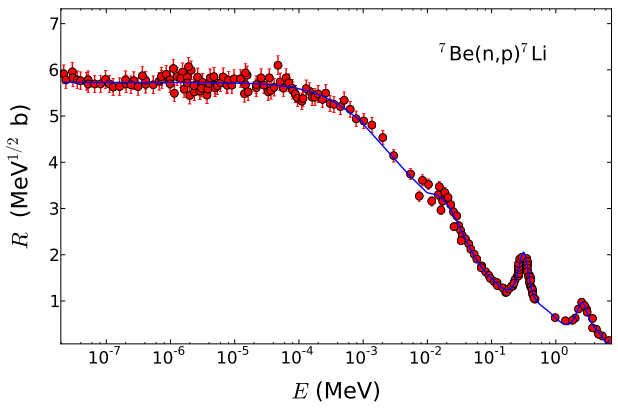

Figure 7: The energy dependence of $R(E) = S(E)\sqrt{E}$ for the reaction ^{7}Be(n,p)^{7}Li. is shown in figure 7. The experimental data were collected from Refs. [28–32]. The solid curve is a function fit to the experimental data using a set of polynomials and Breit-Wigner functions.

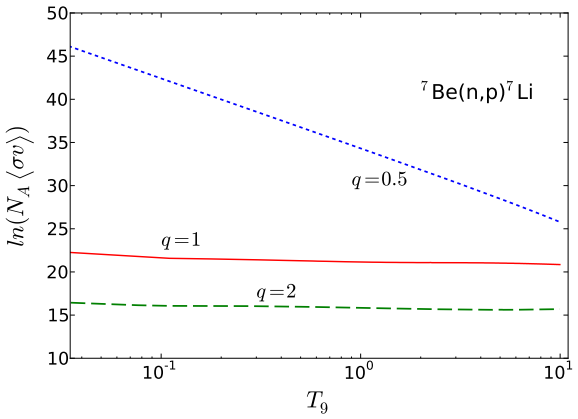

Figure 8: Reaction rates for ^{7}Be(n,p)^{7}Li as a function of the temperature T_9 for two different values of the non-extensive parameter q. The rates are given in terms of the logarithm of $N_A\langle\sigma v\rangle$ (in units of cm^3 mol^{-1} s^{-1}). Results with the use of non-extensive distributions for $q = 0.5$ (dotted line) and $q = 2$ (dashed line) are shown.

particles is the absence of the Coulomb barrier and a correspondingly lack of suppression of the reaction rates at low energies. As the temperature increases, the relative difference between the Maxwell-Boltzmann and the non-Maxwellian distributions decrease appreciably. This will lead to a rather distinctive pattern of the reaction rates for charged compared to neutron induced reactions.

For neutron-induced reactions, a good accuracy (within 0.1%) for the numerical calculation of the reaction rates with Eq. (12) is reached using the integration limits between $E = 0$ and $E = 20k_BT$. As an example we will now consider the reaction ^{7}Be(n,p)^{7}Li. The energy dependence of $R(E) = S(E)\sqrt{E}$ for this reaction is shown in figure 7. The experimental data were collected from Refs. [28–32].

Using the chi-square fit with a sum of polynomials and Breit-Wigners obtained to reproduce the data in figure 7, we show in figure 8 the reaction rates for ^{7}Be(n,p)^{7}Li as a function of the temperature T_9 for different values of the non-extensive parameter q. The rates are given in terms of the natural logarithm of $N_A\langle\sigma v\rangle$ (in units of cm^3 mol^{-1} s^{-1}). The solid curve corresponds to the usual Boltzmann distribution, i.e., $q = 1$. The dashed and dotted curves are obtained for $q = 2$ and $q = 0.5$, respectively. In contrast to reactions induced by charged particles, we now see strong deviations from the Maxwellian rate both for $q > 1$ and $q < 1$. For $q < 1$ the deviations are larger at small temperatures and decrease as the energy increase, tending asymptotically to the Maxwellian rate at large temperatures. This behavior can be understood from figure 6 (for ^{7}Be(n,p)^{7}Li the results are nearly the same as in Fig. 6). At small temperatures, e.g. $T_9 = 0.1$, the distribution for $q = 0.5$ is strongly enhanced at large energies and the tendency is that the reaction rates increase at low temperatures. This enhancement disappears as the temperature increase (lower panel of figure 6). For $q = 2$ the reaction rate is suppressed, although not as much as for the charged-induced reactions, the reason being due a compensation by an increase because of normalization at low energies.

Having discussed the dependence of the reaction rates on the non-extensive parameter q for a few standard reactions, we now consider the implications of the non-extensive statistics to the predictions of the BBN. It is clear from the results presented above that an appreciable impact on the abundances of light elements will arise.

IV. BBN WITH NON-EXTENSIVE STATISTICS

The BBN is sensitive to certain parameters, including the baryon-to-photon ratio, number of neutrino families, and the neutron decay lifetime. We use the values $\eta = 6.19 \times 10^{-10}$, $N_\nu = 3$, and $\tau_n = 878.5$ s for the baryon-photon ratio, number of neutrino families, and neutron-day lifetime, respectively. Our BBN abundances were calculated with a modified version of the standard BBN code derived from Refs. [33–35].

Although BBN nucleosynthesis can involve reactions up to the CNO cycle [36], the most important reactions which can significantly affect the predictions of the abundances of the light elements [^{4}He, D, ^{3}He, ^{7}Li] are n-decay, p(n,γ)d, d(p,γ)^{3}He, d(d,n)^{3}He, d(d,p)t, ^{3}He(n,p)t, t(d,n)^{4}He, ^{3}He(d,p)^{4}He, ^{3}He(α,γ)^{7}Be, t(α,γ)^{7}Li, ^{7}Be(n,p)^{7}Li and ^{7}Li(p,α)^{4}He. Except for these reactions, we have used the reaction rates needed for the remaining reactions from a compilation by NACRE [37] and that reported in Ref. [38]. For

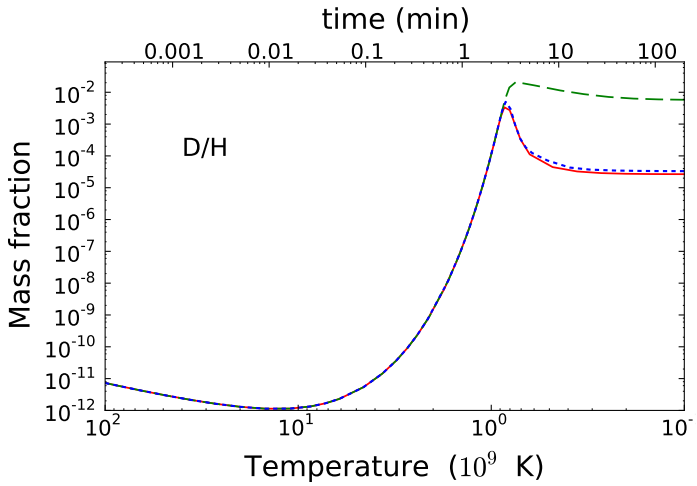

Figure 9: Relative abundances of deuterium to hydrogen. The solid curve is the result with the standard Maxwell distributions for the reaction rates. Results with the use of non-extensive distributions for $q = 0.5$ (dotted line) and $q = 2$ (dashed line) are shown.

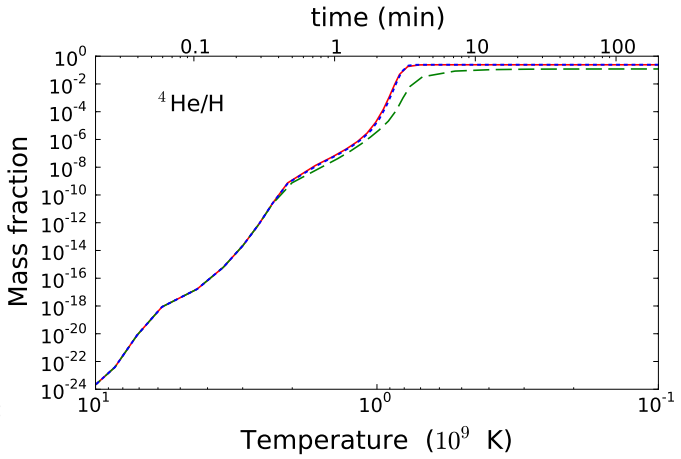

Figure 10: Mass fraction of ^{4}He. The solid curve is the result obtained with the standard Maxwell distributions for the reaction rates. Results with the use of non-extensive distributions for $q = 0.5$ (dotted line) and $q = 2$ (dashed line) are also shown.

the 11 reactions mentioned above, we have collected data from Refs. [37–39], and references mentioned therein, fitted the S-factors with a sum of polynomials and Breit-Wigner functions and calculated the reaction rates for Maxwellian and non-Maxwellian distributions.

In figure 9 we show the calculated relative abundances (or mass fraction) of deuterium to hydrogen. The solid curve is the result with the standard Maxwell distributions for the reaction rates. Using the non-extensive distributions yields the dotted line for $q = 0.5$ and the dashed line for $q = 2$. It is interesting to observe that the deuterium abundances are only moderately modified due to the use of the non-extensive statistics for $q = 0.5$. Up to temperatures of the order of $T_9 = 1$, the mass fraction for D/H tend to agree for the extensive and non-extensive statistics. This is due to the fact that any deuterium that is formed is immediately destroyed (a situation known as the deuterium bottleneck). But, as the temperature decreases, the reaction rates for the p(n,γ)d reaction are considerably enhanced for $q = 2$ (see figure 6), and perhaps more importantly, they are strongly suppressed for all other reactions involving deuterium destruction, as clearly seen in figure 3. This creates an unexpected over abundance of deuterons for the non-extensive statistics with $q = 2$. The existence of deuterium at a low but constant primordial fraction in all hydrogen, is one of the arguments in favor of the big bang theory of the universe. It is estimated that the abundances of deuterium have not evolved significantly since their production about 13.7 billion years. The predictions for the D/H ratio for the $q = 2$ statistics (D/H $= 5.70 \times 10^{-3}$) is about a factor 200 larger than those from the standard BBN model, also clearly in disagreement with the observation, $\sim 2.8{\times}10^{-5}$ [5].

Table I: Predictions of the BBN (with $\eta_{WMAP} = 6.2 \times 10^{-10}$) with Maxwellian and non-Maxwellian distributions compared with observations. All numbers have the same power of ten as in the last column.

	Maxwell BBN	Non-Maxwell $q = 0.5$	Non-Maxwell $q = 2$	Observation
^{4}He/H	0.249	0.243	0.141	0.249
D/H	2.62	3.31	570	$2.82{\times}10^{-5}$
^{3}He/H	0.98	0.91	69.1	$(0.9 - 1.3){\times}10^{-5}$
^{7}Li/H	4.39	6.89	356.	1.1×10^{-10}

A much more stringent constraint for elemental abundances is the mass fraction of ^{4}He, which observations set at about 25% [40]. The ^{4}He mass fraction generated from a BBN calculation is plotted in figure 10. The solid curve is the result obtained with the standard Maxwell distributions for the reaction rates. Using the non-extensive distributions yields the dotted line for $q = 0.5$ and the dashed line for $q = 2$. Again, the predicted abundances for $q = 2$ deviate substantially from standard BBN results. This time only about half of ^{4}He is produced with the use of a non-extensive statistics with $q = 2$. The reason is the suppression of the reaction rate for formation of ^{4}He for $q = 2$ from the charged particle reactions t(d,n)^{4}He, ^{3}He(d,p)^{4}He.

A strong impact of using non-extensive statistics for both $q = 0.5$ and $q = 2$ values of the non-extensive parameter is seen in figure 11 for the ^{3}He mass fraction.

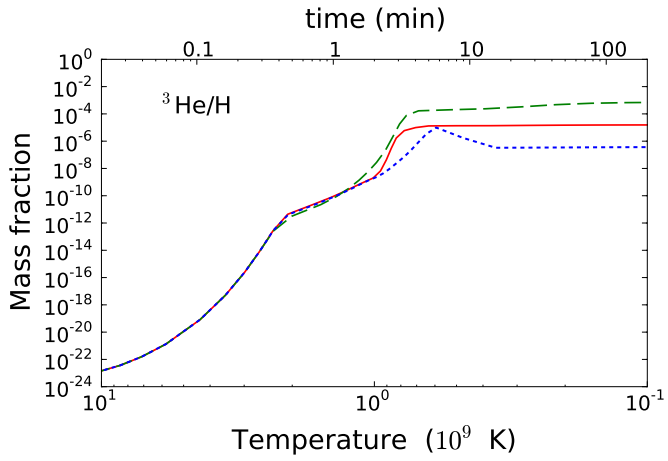

Figure 11: Mass fraction of ^{3}He. The solid curve is the result obtained with the standard Maxwell distributions for the reaction rates. Results with the use of non-extensive distributions for $q = 0.5$ (dotted line) and $q = 2$ (dashed line) are also shown.

While for $q = 2$ there is an overshooting in the production of ^{3}He, for $q = 0.5$ one finds a smaller value than the one predicted by the standard BBN. This is due to the distinct results for the destruction of ^{3}He through the reaction ^{3}He(n,p)t, which is enhanced for $q = 0.5$ and suppressed for $q = 2$, in the same way as it happens for the reaction ^{7}Be(n,p)^{7}Li, shown in figure 7.

V. CONCLUSIONS

In table I we present our results for the predictions of the BBN with Maxwellian and non-Maxwellian distributions. The predictions are compared with the results from observations reported in the literature. It is evident that the results obtained with the non-extensive statistics strongly disagree with the experimental data. The overabundance of ^{7}Li compared to observation gets worse if $q > 1$. The three light elements D, ^{4}He and ^{7}Li have well-measured primordial abundances. For all these abundances, a non-extensive statistics with $q > 1$ leads to a great discrepancy with the experimental data.

Except for the case of ^{3}He the use of non-extensive statistics with $q < 0.5$ does not rule out its validity when the non-Maxwellian BBN results are compared to observations. ^{3}He is at present only accessible in our Galaxys interstellar medium. This means that it cannot be measured at low metallicity, a requirement to make a fair comparison to the primordial generation of light elements. This also means that the primordial ^{3}He abundance cannot be determined reliably. The result presented for the ^{3}He abundance in table I is quoted from Ref. [41].

We conclude that it does not seem possible to change the Maxwell-Boltzmann statistics to reproduce the observed abundance of light elements in the universe without destroying many other successful predictions of big bang nucleosynthesis. We have calculated a window of opportunity for the non-extensive parameter q with which one can reproduce the observed abundance of light elements. From a chi-square fit of our results with the observed abundances we conclude that window to be $q = 1^{+0.04}_{-0.1}$. This means that, should a non-Maxwellian distribution due to the use of the Tsallis non-extensive statistics be confirmed (with a sizable deviation from $q = 1$), our understanding of the cosmic evolution of the universe will have to be significantly changed.

This work was partially supported by the US-DOE grants DE-FG02-08ER41533 and DE-FG02-10ER41706, and by the Brazilian agencies, CNPq and FAPESP. One of the authors (C.B.) acknowledges the Helmholtz International Center for FAIR (HIC for FAIR) for supporting his visit to the GSI Helmholtzzentrum für Schwerionenforschung, where much of this work was done.

[1] P. Noterdaeme, P. Petitjean, R. Srianand, C. Ledoux, and S. Lopez, Astron. and Astrophys. 526, L7 (2011).
[2] LEP Collaboration, Phys. Rep. 427, 257 (2006).
[3] Fred E. Wietfeldt and Geoffrey L. Greene, Rev. Mod. Phys. 83, 1173 (2011).
[4] E. Komatsu, et al., ApJS 192, 18 (2011).
[5] Brian D. Fields, Ann. Rev. Nucl. Part. Sci. 61, 47 (2011).
[6] C. Tsallis, J. Stat. Phys. 52, 479 (1988).
[7] "Introduction to Nonextensive Statistical Mechanics", C. Tsallis, Springer Verlag (2009), ISBN 978-0-387-85358-1.
[8] R. Silva Jr., A.R. Plastino, and J. Lima, Phys. Lett. A249, 401 (1998).
[9] J.A. S. Lima, R. Silva Jr., and J. Santos, Phys. Rev. E61, 3260 (2000).
[10] V. Muñoz, Nonlin. Processes Geophys. 13, 237 (2006).
[11] W.A. Fowler, G.R. Caughlan, and B.A. Zimmerman, Ann. Rev. Astron. Astrophys. 5, 525 (1967).
[12] R.L. Schulte, M. Cosack, A.W. Obst, J.L. Weil, Nucl. Phys. A192, 609 (1972).
[13] A. Krauss, H.W. Becker, H.P. Trautvetter, C. Rolfs, K. Brand, Nucl. Phys. A465, 150 (1987). [
[14] R.E. Brown, N. Jarmie, Phys. Rev. C41, 1391 (1990).
[15] H.-S. Bosch, G.M. Hale, Nucl. Fusion 32, 611 (1992).
[16] U. Greife, F. Gorris, M. Junker, C. Rolfs, D. Zahnow, Z. Phys. A351, 107 (1995).
[17] J. M. Freeman, R. C. Hanna and J. H. Montague, Nucl. Phys. 5 (1958) 148.
[18] Y. Cassagnou, J. M. Jeronymo,G. S. Mani, A. Sadeghi and P. D. Forsyth, Nucl. Phys. 33 (1962) 449.
[19] Y. Cassagnou, J. M. Jeronymo,G. S. Mani, A. Sadeghi

and P. D. Forsyth, Nucl. Phys. 41 (1963) 176
[20] G. S. Mani, R. Freeman, F. Picard, A. Sadeghi and D. Redon, Nucl. Phys. 60 (1964) 588.
[21] O. Fiedler and P. Kunze, Nucl. Phys. A96 (1967) 513.
[22] G. M. Lerner and J. B. Marion, Nucl. Inst. Meth. 69 (1969) 115.
[23] H. Spinka, T. Tombrello and H. Winkler, Nucl. Phys. A164 (1971) 1.
[24] C. Rolfs and R. W. Kavanagh, Nucl. Phys. A455 (1986) 179.
[25] J. F. Harmon, Phys. Rev. C8 (1973) 106.
[26] S. Engstler, G. Raimann, C. Angulo, U. Greife, C. Rolfs, U. Schröder, E. Somorjai, B. Kirch and K. Langanke, Z. Phys. A342 (1992) 471.
[27] S. Engstler, G. Raimann, C. Angulo, U. Greife, C. Rolfs, U. Schröder, E. Somorjai, B. Kirch and K. Langanke, Phys. Lett. B279 (1992) 20.
[28] J.H. Gibbons, R.L. Macklin, Phys. Rev. 114 (1959) 571.
[29] R.R. Borchers, C.H. Poppe, Phys. Rev. 129 (1963) 2679.
[30] K.K. Sekharan, H. Laumer, B.D. Kern, F. Gabbard, Nucl. Instrum. Methods 133 (1976) 253.
[31] C.H. Poppe, J.D. Anderson, J.C. Davis, S.M. Grimes, C. Wong, Phys. Rev. C 14 (1976) 438.
[32] P.E. Koehler, C.D. Bowman, F.J. Steinkruger, D.C. Moody, G.H. Hale, J.W. Starner, S.A. Wender, R.C. Haight, P.W. Lisowski, W.L. Talbert, Phys. Rev. C 37 (1988) 917.
[33] Robert Wagoner, William A. Fowler, and F. Hoyle, Astrophys. J. 148, 3 (1967).
[34] L. Kawano (1988), FERMILAB Report No. PUB-88/34-A (unpublished).
[35] L. Kawano, NASA STI/Recon Technical Report N 92, 25163 (1992).
[36] Alain Coc, Stephane Goriely, Yi Xu, Matthias Saimpert, and Elisabeth Vangioni, arXiv:1107.1117.
[37] C. Angulo et al., Nucl. Phys. A 656, 3 (1999).
[38] P. Descouvemont, A. Adahchour, C. Angulo, A. Coc,, and E. Vangioni-Flam, At. Data Nucl. Data Tables 88, 203 (2004).
[39] M.S. Smith, L.H. Kawano, R.A. Malaney, Astrophys. J. Suppl. 85 (1993) 219.
[40] A.M. Boesgaard, and G. Steigman, Ann. Rev. Astron. Astrophys. 23, 319 (1985).
[41] T. Bania, R. Rood and D. Balser, Nature 415, 54 (2002).